Mechanical deformation study of copper nanowire using atomistic simulation

2001 Nanotechnology 12 295

(http://iopscience.iop.org/0957-4484/12/3/317)

INSTITUTE OF PHYSICS PUBLISHING NANOTECHNOLOGY
Nanotechnology **12** (2001) 295–300 PII: S0957-4484(01)21319-1

Mechanical deformation study of copper nanowire using atomistic simulation

Jeong-Won Kang and Ho-Jung Hwang

Semiconductor Process and Device Laboratory, Department of Electronic Engineering, Chung-Ang University, 221 HukSuk-Dong, DongJak-Ku, Seoul 156-756, Korea

E-mail: kok@semilab3.ee.cau.ac.kr

Received 23 January 2001, in final form 8 July 2001
Published 24 August 2001
Online at stacks.iop.org/Nano/12/295

Abstract
We investigated mechanical deformations of Cu{100} nanowires using the steepest-descent method. We simulated the cases of elongation, shearing, rotation and rotated elongation. Before the first yielding nanowires preserve the elastic stage, and after this mechanical deformations proceed in alternating quasi-elastic and yielding stages. In the case of rotation deformation, the torque was inversely proportional to the tension force. It was shown that a nanowire in the case of rotated elongation is deformed more easily than one in cases of both elongation and rotation.

1. Introduction

The properties of condensed systems with nanometre dimensions have been investigated actively in the past decade [1]. The continuing miniaturizations of electronic devices and nanoscale measurement systems have stimulated an interest in nanometre-scale materials such as nanowires and point contacts [2–29]. Metallic nanowires have received considerable attention in relation to wiring in nanometre-scale integrated circuits of the future [20–26] and for tips of scanning tunnelling microscope (STM) and atomic force microscope (AFM) operation under nanoscale tip–sample interaction [27–30]. Most authors have investigated and simulated Au nanowires [2–5, 11–15]. Mehrez and Ciraci investigated the yielding and fracturing mechanisms of Cu nanowires as functions of the stretch velocities by using classical molecular dynamics simulation [19]. However, since they investigated only elongation of Cu nanowires and used narrow Cu nanowires with five atomic layers, each of which had 12 or 13 atoms, their work was not enough to understand the fracture mechanism of Cu nanowires. In our previous work [31], we studied elongation and shearing deformations of Cu nanowires with stretch velocity and nanowire diameter using classical molecular dynamics simulations. Our previous work presented the result that as the stretch velocity increased, the strain causing the first yield decreased, the period of yielding was shortened, the strain causing the rupture decreased and the magnitudes of the force relaxation decreased. In the case of the larger-diameter nanowire, the nanowire region, which was originally {100} planes, became a quasi-cylindrical nanowire with {111} surface. However, in our previous work other mechanical deformations, such as rotation, were not investigated. For applications of Cu nanostructures of the future, an understanding of various deformation mechanisms is necessary.

In this paper, using the steepest-descent (SD) method, we study mechanical deformations of Cu nanowires, such as elongation, shearing, rotation and rotated deformations. The yielding, rearrangement, structural transition and mechanisms of fracture of Cu nanowires by an external agent are investigated.

2. Simulation procedure

We consider rectangular nanowires cut from bulk Cu, as figure 1 shows. The wire has two ends, that are connected by a neck, which consists of ten atomic layers perpendicular to the wire axis [001] and is put between the top and bottom layers. Each atomic layer has 18 atoms. A stable atomic configuration after deformation was calculated by the SD method. The bottom and the top layers are labelled as B and T, respectively. It is possible to assume that the breaking is governed by phenomena occurring at the central part of the nanowires. Therefore the atoms in these layers are fixed during simulations, and we apply the SD method to atoms in the nanowire region labelled as N. In a previous study on Au nanowires, Tanimori and Shimamura applied the Monte Carlo method to the atoms in region N [11]. For Cu, we use the potential function of the second-moment approximation of the tight-binding (SMA-TB) scheme [32, 33].

Table 1. The SMA-TB results are compared to results of a simple analytic nearest-neighbour embedded-atom model developed by Johnson [42] and Baskes [43]. The SMA-TB results of the surface diffusion barrier are compared with other results, such as effective medium (EM) [45, 46], corrected effective medium (CEM) [47], embedded-atom models in the Voter–Chen parametrization (EA(VC)) [48] and in the Adams–Foiles–Wolfer parameterization (EA(AFW)) [49], *ab initio* density-functional calculations in the local-density approximation (LDA) [50], *ab initio* density-functional results with gradient corrections (GGA) [50] and experimental results [51]. E_c and a_0 are the cohesive energy of atom and lattice constant, respectively.

			Energy/atom on surface (eV)			Energy/atom on surface (eV)		
	E_c(eV)	a_0(Å)	(100)	(110)	(111)	Surface	Edge	Inside
SMA-TB	−3.544	3.615	−2.999	−2.913	−3.127	−2.999	−2.547	−3.548
EAM-I	−3.540	3.620	−2.989	−2.848	−3.064	−2.989	−2.499	−3.451
EAM-II	−3.540	3.620	−2.360	−2.065	−2.655	−2.360	−1.475	−3.540
	SMA-TB	EM	CEM	EA(VC)	EA(AFW)	LDA	GGA	Experiment
			Diffusion barriers on (100) surface (eV)					
Jump	0.41	0.40[b]	0.47[d]	0.53[f]	0.38[f]	0.65–0.75[g]	0.51–0.55[g]	0.39 ± 0.06[h]
Exchange	0.79	—	0.43[d]	0.79[f]	0.72[f]	1.03–1.23[g]	0.82–0.96[g]	—
			Diffusion barriers on (110) surface (eV)					
In channel	0.23[a]	0.29[c]	0.26[e]	0.53[f]	0.24[f]	—	—	—
Cross channel	0.29[a]	0.56[c]	0.49[e]	0.31[f]	0.30[f]	—	—	—

[a] [44]. [b] [45]. [c] [46]. [d] [47]. [e] [48].[f] [49]. [g] [50]. [h] [51].

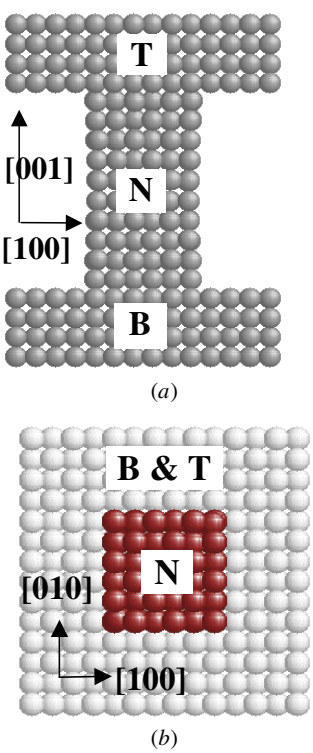

Figure 1. Simulated Cu nanowire structure: (*a*) the side view and (*b*) the top view. The bottom and top layers are labelled B and T, respectively. The atoms in these layers are fixed during simulations. The layers labelled by N are nanowire regions. Molecular dynamics is applied to atoms in region N.

(This figure is in colour only in the electronic version)

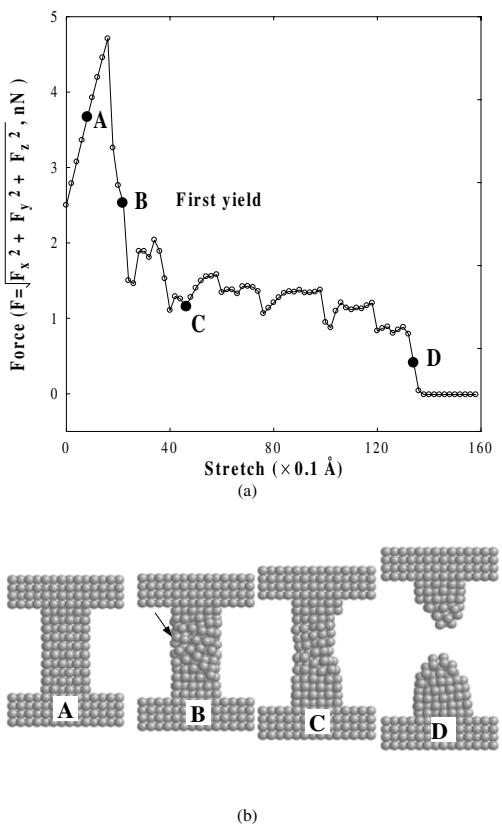

Figure 2. A Cu nanowire was composed of ten atomic layer, each of which has 18 atoms. A stable atomic configuration was calculated by the SD method. (*a*) The variation of tensile force with the elongation along the z-axis for a Cu nanowire. (*b*) Atomic arrangements at points A–D in figure 2(*a*). The arrow denotes the slip [110] direction.

The SMA-TB type potential function has been used in atomistic simulation studies of nanoclusters [34–38] and ultrathin nanowires [39]. Table 1 shows the physical values calculated by SMA-TB and other theoretical methods and measured by experiment, and these values calculated by SMA-TB are in agreement with the other results.

The initial atomic arrangement in the wire is relaxed by the SD method. Since we use the SD method, the thermal effects and temperature-dependent deformation mechanisms are not included in this paper. We simulate the elongation, shearing

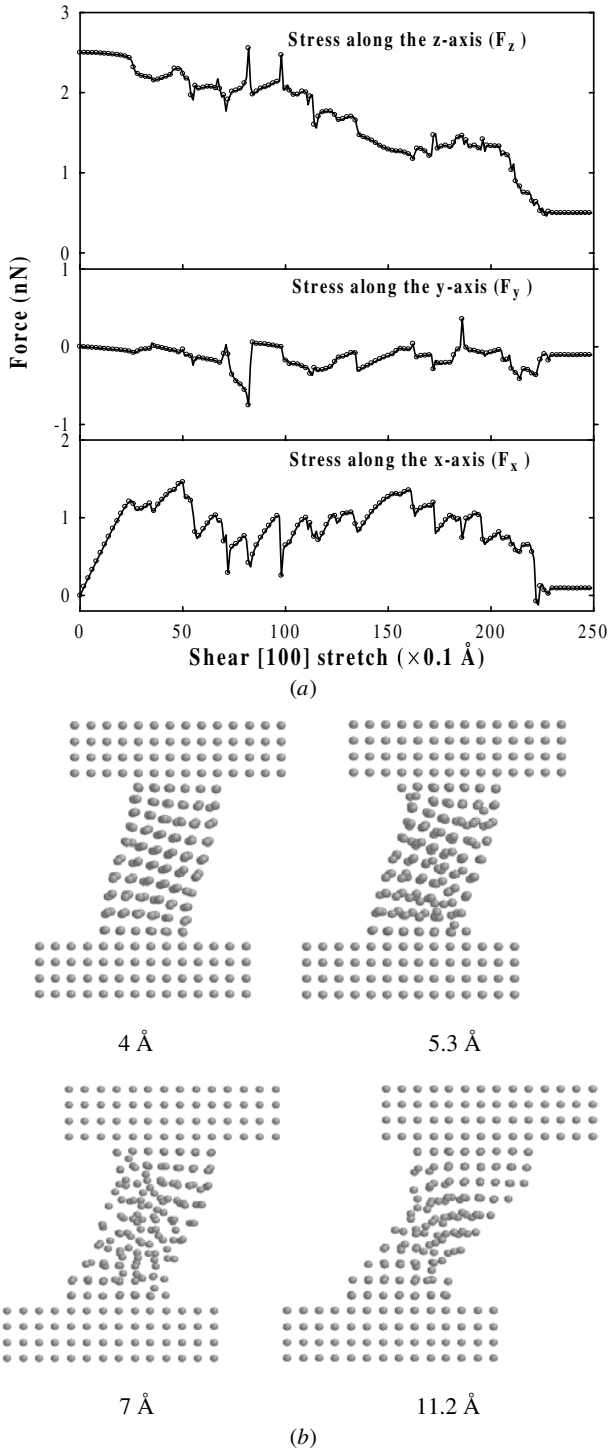

Figure 3. (*a*) The variation of shear force with the shearing along the [100] direction for a Cu nanowire. (*b*) Atomic arrangements at the shearing point 4, 5.3, 7 and 11.2 Å.

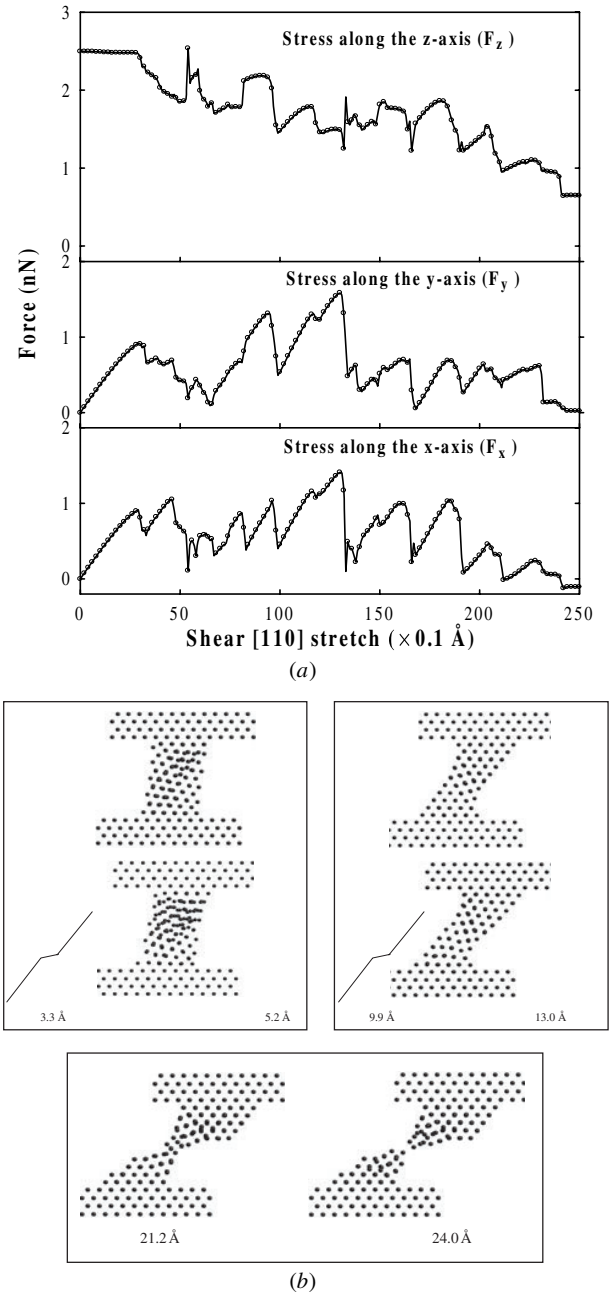

Figure 4. (*a*) The variation of shear force with the shearing along [110] for a Cu nanowire. (*b*) Atomic arrangements at the shearing point 3.3, 5.2, 9.9, 13.0, 21.2 and 24.0 Å.

and rotation of the Cu nanowires. In elongation, the distance between the top and the bottom layers is slightly stretched. The top layers are displaced along the [001] direction in increments of 0.1 Å. In [100] and [110] shears, the top layer is displaced in the [100] and [110] directions with increment 0.1 Å. In rotation, the top layer rotates through 1° in the centre of the top layer. After a small deformation, the atomic arrangement in the nanowires is relaxed. Such small deformation and relaxation are repeated. The tensile and shear forces, that correspond to the force exerted by the pulling agent on the wire, are the attractive force between the top-layer region and the nanowire region and are calculated after relaxation. In this paper, [100], [010] and [001] directions are the *x*-, *y*- and *z*-axes, respectively.

3. Simulation results

We present the results of mechanical deformation simulations of the Cu nanowire. Figure 2(*a*) shows the variation of tensile force with elongation. Figure 2(*b*) shows the stable atomic

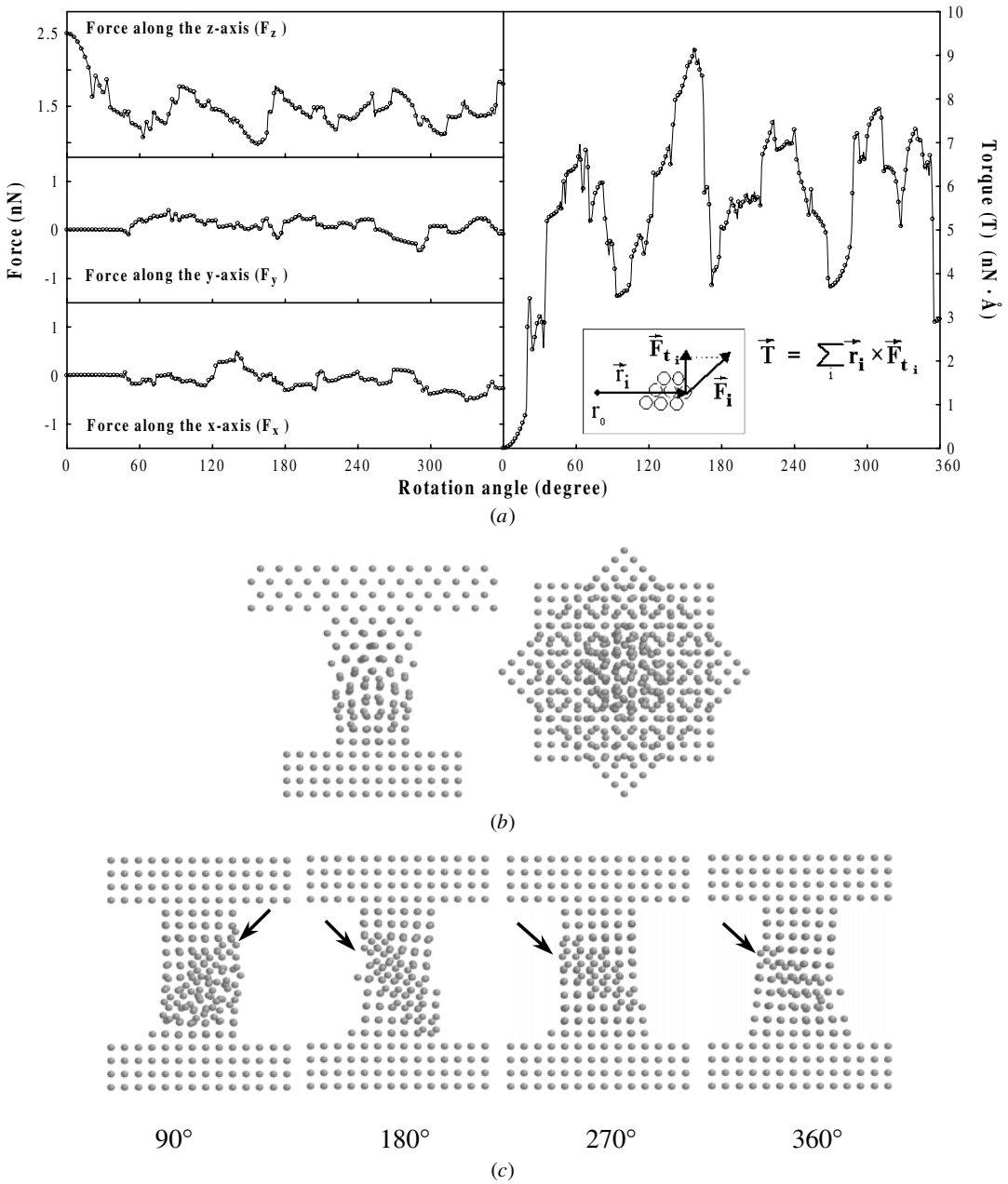

Figure 5. (*a*) Forces and torque variations as a function of rotation angle. (*b*) [100] and [001] side views at 45°. (*c*) Atomic arrangements of [100] view at the rotation angle 90°, 180°, 270°, and 360°.

configuration at points A–D in figure 2(*a*). At point A, the number of atomic layers is still ten, and the wire elongates uniformly. The point A is in the elastic range. When the strain ($\Delta L/L$) is 0.133 (the stretch is 2.4 Å), the first yield occurs (point B in figure 2). The first yield is related to an abrupt slipping event on the {111} plane. The arrow in figure 2(*b*) denotes the slip direction. The slip caused by an external force preferentially occurs when the least amount of energy is consumed. This condition is fulfilled when the slips occur in ⟨110⟩ directions on the {111} plane in bulk FCC materials [40] and $(1/2)\langle 110\rangle\{111\}$ dislocations split into partial dislocations with Burger vectors $(1/6)\langle 211\rangle$ [41]. However, nanowire deformation mechanisms include various dislocation slips, and at least two distinct slip mechanisms mainly affect nanowire deformation processes [16]. One is a glide of a dislocation on {111} planes and the other is a homogeneous slip of one plane of atoms over another plane of atoms. The crossover of the two slip mechanisms is related to reduction of diameter of the nanowire centre. Whenever diameters of nanowires in elongation cases abruptly reduce, homogeneous slips appear. When the strain is 0.752 (the stretch is 13.8 Å), the rupture occurs (point D in figure 2). After the first yielding, the elongation deformation proceeds in alternating quasi-elastic and yielding stages. Whenever yielding occurs, the atomic structure is disordered, the original stacking sequence is deformed, the neck is narrowed more and more and the tensile force decreases abruptly. The magnitude of force relaxation (the decrease of the tensile force) at the first

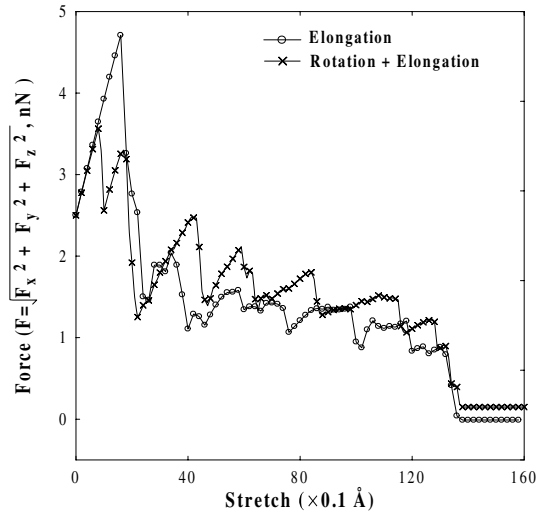

(a)

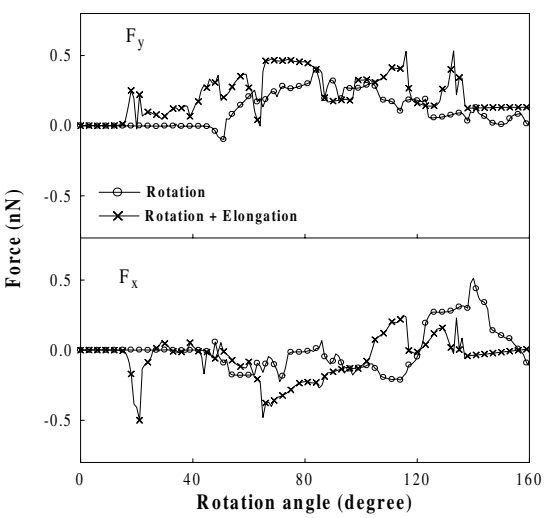

(b)

Figure 6. (*a*) Comparison of total forces between elongation and rotated elongation. (*b*) Comparison of the shearing stresses between rotation and rotated elongation.

yield is 3.26 nN in this paper. At the other yields except the first yield, the magnitude of force relaxation is below 1 nN. These values are in agreement with the previous result [19]. The overall behaviour of tensile force, F, is in agreement with the experimental results [3, 8, 9].

Next we simulated the [100] direction shear deformation of a Cu nanowire. Figure 3 shows forces along the x-, y- and z-axis directions and atomic configurations with deformations of the Cu nanowire. The initial value of F_z starts at 2.5 nN because the fixed top layers have a larger area than the nanowire region in our simulation as in [19], and as shear stretch proceeds the F_z decreases. The values of F_x and F_y start at 0 nN. During shearing, the average of F_y is near 0 nN and F_y deviated from zero at the yielding points. In the variation of F_x, the shear deformation also proceeds in alternating quasi-elastic and yielding stages. As the shear stretch increases, the atomic structure becomes disordered, and the original stacking sequence is deformed. At yielding, the tensile force decreases abruptly. During shear stretch, the nanowire remains mainly in the {100} structure, except when temporary states such as {111} planes are found during atomic rearrangement. While the reduction of the number of atomic layers was found in the previous simulation study for shear of Au {111} nanowires [11], the number of atomic layers in this paper remains at ten. In the previous work using classical molecular dynamics simulation, we investigated that the homogeneous slips without following slips on the {111} planes during the shearing deformation of thin Cu{100} nanowire with high shearing velocity. In this paper, using the SD method, at first the ⟨110⟩ direction slip occurs, and next a homogeneous slip follows. The first slip occurs in the $[10\bar{1}]$ direction with a dislocation glide slip mechanism. Temporary states with {111} planes are found during structure rearrangement before yielding, and then slips occur in the ⟨110⟩ directions. After that, the Cu nanowire swiftly rearranges in the {100} planes to the original structure. The nanowire is broken at 22.1 Å.

We simulated the [110] direction shear deformations of a Cu nanowire. Figure 4 shows forces and atomic configurations for the Cu nanowire during the [110] direction shear deformations. As shear stretch proceeds, the F_z decreases. Variation of F_z in this case is similar to that of the previous case. However, the variation of F_x is similar to F_y. The shear deformations proceed in alternating quasi-elastic and yielding stages. Properties of slip directions in this case are the same as the previous cases. The first yielding point occurs at 3.3 Å. In an atomic configuration after several yields, at 9.9 Å, stacking faults in an FCC Cu nanowire with a small twinned region appear. The structure with the small twinned region remains until the next yielding point, 13 Å. The nanowire is broken at 24 Å, longer than 22.1 Å in the above [100] shearing case.

Next we simulated the rotation deformation of a Cu nanowire. Figure 5 shows forces, torque and atomic configurations at the rotation angles for the Cu nanowire during the rotation deformations. Until the rotation angle is 45°, atomistic arrangements keep a symmetrical structure with the nanowire centre such as that shown in figure 5(*b*). Therefore, until 45° the net force of the xy plane (perpendicular plane of the nanowire axis) is zero but the torque of the xy plane (T) increases. In figure 5(*a*), we can see that T is inversely proportional to F_z. Figure 5(*c*) shows atomistic arrangements with the rotation angles, and arrows in figure 5(*c*) indicate the ⟨110⟩ slip directions.

Next we simulated the rotated elongation of a Cu nanowire. An elongation of 0.1 Å and a rotation through 1° of the top layer deform the nanowire. The total force variation of rotated elongation is compared with that of elongation in figure 6(*a*). The shearing force variations of rotated elongation are compared with that of rotation in figure 6(*b*). The first yield strain in the case of rotated elongation is one-half of that in the elongation case. Shear forces in the case of rotated elongation appear at 16° after the first yield. Therefore, we can see that the nanowire in the case of rotated elongation is deformed more easily than that in cases of both elongation and rotation.

4. Summary

We have investigated the mechanical deformations of Cu{100} nanowires. We simulated the cases of elongation, shearing, rotation and rotated elongation. Before the first yielding nanowires preserved the elastic stages, and after this the mechanical deformation proceeded in alternating quasi-elastic and yielding stages. For Cu thin {100} nanowires in this paper, the crossover between the [110] direction slip on the {111} planes and the homogeneous slip occurred in cases of elongation, shearing and rotated elongation. In the case of rotation deformation, until the rotation angle was 45°, since atomistic arrangements kept a symmetrical structure with the nanowire centre, the net force in the xy plane was zero. However until 45° the torque of xy plane increased, and it was shown that T was inversely proportional to F_z. The first yield strain in the case of rotated elongation was one-half of that in the elongation case, and shear forces in the case of rotated elongation appeared at 16° after the first yield.

The present simulation study shows some of the yielding and fracturing mechanisms for Cu nanowires. For the metallic nanowires and nanocontacts related in this paper several research opportunities remain. Further research will, therefore, include more detailed effects of size, shape, thermal and crystal orientation of nanowires and will deal with screwed stresses, compression, shear velocity direction etc.

References

[1] Beeby J L (ed) 1991 *Condensed Systems of Low Dimension, NATO Advanced Study Institute Series B253: Physics* (New York: Plenum)
Leo Esaki (ed) 1991 *Highlights in Condensed Matter Physics and Future Prospects, NATO Advanced Study Institute Series B285: Physics* (New York: Plenum)

[2] Sutton A P and Pethica J B 1990 *J. Phys.: Condens. Matter* **2** 5317

[3] Landman U, Luedtke W D, Burnham N A and Colton R J 1990 *Science* **248** 454
Landman U and Luedtke W D 1991 *J. Vac. Sci. Technol* B **9** 414
Landman U, Luedtke W D, Salisbury B E and Whetten R L 1996 *Phys. Rev. Lett.* **77** 1362

[4] Pascual J I, Mendez J, Gomez-Herrero J, Baro A M, Garcia N and Binh V T 1993 *Phys. Rev. Lett.* **71** 1852
Pascual J I, Mendez J I, Gomez-Herrero J, Baro A M, Garcia N, Landman U, Luedtke W D, Bogachek E N and Cheng H P 1995 *Science* **267** 1793
Pascual J I, Mendez J, Gomez-Herrero J, Baro A M, Garcia N, Landman U, Luedtke W D, Bogachek E N and Cheng H P 1995 *J. Vac. Sci. Technol* B **13** 1280

[5] Olesen L, Laegsgaard E, Stensgaard I, Besenbacher F, Shiotz J, Stoltze P, Jacobsen K W and Norskov J K 1994 *Phys. Rev. Lett.* **72** 2251
Olesen L, Laegsgaard E, Stensgaard I, Besenbacher F, Shiotz J, Stoltze P, Jacobsen K W and Norskov J K 1995 *Phys. Rev. Lett.* **74** 2147

[6] Ciraci S and Tekman E 1989 *Phys. Rev.* B **40** 11969

[7] Krans J M, Muller C J, Yanson I K, Govaert T C M, Hesper R and Van Ruitenbeek J M 1994 *Phys. Rev.* B **48** 14721
Krans J M, Muller C J, van der Post N, Postma F R, Sutton A P, Todorov T N and Van Ruitenbeek J M 1995 *Phys. Rev. Lett.* **74** 2146

[8] Agrait N, Rubio G and Vieira S 1995 *Phys. Rev. Lett.* **74** 3995
Rubio G, Agarit N and Vieira S 1996 *Phys. Rev. Lett.* **76** 2302

[9] Stalder A and Durig U 1996 *Appl. Phys. Lett.* **68** 637

[10] Dubois S, Piraux L, George J M, Ounadjela K, Duvail J L and Fert A 1999 *Phys. Rev.* B **60** 477

[11] Tanimori S and Shimamura S 2000 *Tech. Proc. 3rd Int. Conf. on Modeling and Simulation of Microsystems, MSM2000 (San Diego, CA, 2000)* p 110

[12] Sorensen M R, Brandbyge M and Jacobsen K W 1998 *Phys. Rev.* B **57** 3283

[13] Hansen K, Laegsgaard E, Stensgarrd I and Besenbacher F 1997 *Phys. Rev.* B **56** 2208

[14] Correia A and Garcia N 1997 *Phys. Rev.* B **55** 6689

[15] Bilalbegovic G 1998 *Phys. Rev.* B **58** 15412

[16] Sorensen M R, Jacobsen K W and Stoltze P 1996 *Phys. Rev.* B **53** 2101

[17] Todorov T M and Sutton A P 1993 *Phys. Rev. Lett.* **70** 2138

[18] Lynden-Bell R M 1994 *Science* **263** 1704

[19] Mehrez H and Ciraci S 1997 *Phys. Rev.* B **56** 12 632

[20] Cleland A N and Roukes M L 1998 *Nature* **392** 160

[21] Huang Y, Duan X, Wei Q and Lieber C M 2001 *Science* **291** 630

[22] Cui Y and Lieber C M 2001 *Science* **291** 851

[23] Duan X, Huang Y, Cul Y, Wang J and Lieber C M 2001 *Nature* **409** 66

[24] Bezryadin A, Lau C N and Tinkham M 2000 *Nature* **404** 971

[25] Okawa Y and Aono M 2001 *Nature* **409** 684

[26] Chung S W, Yu J Y and Heath J R 2000 *Appl. Phys. Lett.* **76** 2068

[27] Dai H, Hafner J H, Rinzler A G, Colbert D T and Smalley R E 1996 *Nature* **384** 147

[28] Dai H, Franklin N and Han J 1998 *Appl. Phys. Lett.* **23** 1508

[29] Bouhacina T, Aime J P, Gauthier S and Michanl D 1997 *Phys. Rev.* B **56** 7694

[30] Akita S, Nishijima H and Nakayama Y 2000 *J. Phys. D: Appl. Phys.* **33** 2673

[31] Kang J W and Hwang H J 2001 *J. Korean Phys. Soc.* **38**

[32] Tomanek D, Aligia A A and Balseiro C A 1985 *Phys. Rev.* B **32** 5051

[33] Cleri F and Rosato V 1993 *Phys. Rev.* B **48** 22

[34] Michaclian K, Rendon N and Garzon I L 1999 *Phys. Rev.* B **60** 2000

[35] Palacios F J, Iniguez M P, Lopez M J and Alonso J A 1999 *Phys. Rev.* B **60** 2908

[36] Rongwu L, Ahengying P and Yukun H 1996 *Phys. Rev.* B **53** 4156

[37] Li T X, Yin S Y, Ji Y L, Wang B L, Wang G H and Zhao J J 2000 *Phys. Lett.* A **267** 403

[38] Lei H 2001 *J. Phys.: Condens. Matter* **13** 3023

[39] Wang B, Yin S, Wang G and Zhao J 2001 *J. Phys.: Condens. Matter* **13** L403

[40] Hummel R E 1998 *Understanding Materials Science: History, Properties, and Application* (New York: Springer) ch 4

[41] Shenoy V B, Kukta R V and Phillips R 2000 *Phys. Rev. Lett.* **84** 1491

[42] Johnson R A 1989 *Phys. Rev.* B **39** 12554

[43] Baskes M A 1992 *Phys. Rev.* B **46** 2727

[44] Montalenti F and Ferrando R 1999 *Phys. Rev.* B **59** 5881

[45] Merikoski J, Vattulainen I, Heinonen J and Ala-Nissila T 1997 *Surf. Sci.* **387** 167
Merikoski J and Ala-Nissila R 1995 *Phys. Rev.* B **52** 8715

[46] Stolze P 1994 *J. Phys.: Condens. Matter* **6** 9495

[47] Perkins L S and DePristo A E 1993 *Surf. Sci.* **294** 67

[48] Perkins L S and DePristo A E 1994 *Surf. Sci.* **317** L1152

[49] Lui C J, Cohen J M, Adams J B and Voter A F 1991 *Surf. Sci.* **253** 334

[50] Boisvert G and Lewis L J 1997 *Phys. Rev.* B **56** 15569

[51] Breeman M and Boerma D O 1992 *Surf. Sci.* **269-170** 224